HIV-1 evolutionary dynamics under non-suppressive antiretroviral therapy.

Steven A Kemp[1,3], Oscar Charles[1], Anne Derache[2], Collins Iwuji [2,5], John Adamson[2], Katya Govender[2], Tulio de Oliveira[2,6], , Nonhlanhla Okesola[2], Francois Dabis[7,8], on behalf of the French National Agency for AIDS and Viral Hepatitis Research (ANRS) 12249 Treatment as Prevention (TasP) Study Group, Deenan Pillay[1], Darren P Martin[9], Richard A. Goldstein[1] & Ravindra K Gupta[2,3]

1. Division of Infection & Immunity, University College London, London, UK
2. Africa Health Research Institute, Durban, South Africa
3. Cambridge Institute of Therapeutic Immunology & Infectious Disease (CITIID), Cambridge, UK
4. Department of Medicine, University of Cambridge, Cambridge, UK
5. Research Department of Infection and Population Health, University College London, United Kingdom.
6. KRISP - KwaZulu-Natal Research and Innovation Sequencing Platform, UKZN, Durban, South Africa.
7. INSERM U1219-Centre Inserm Bordeaux Population Health, Université de Bordeaux, France.
8. Université de Bordeaux, ISPED, Centre INSERM U1219-Bordeaux Population Health, France.
9. Department of Integrative Biomedical Sciences, University of Cape Town, South Africa

Address for correspondence:
Ravindra K. Gupta
Cambridge Institute for Therapeutic Immunology and Infectious Diseases
Jeffrey Cheah Biomedical Centre
Puddicombe Way
Cambridge CB2 0AW, UK
Rkg20@cam.ac.uk

Or

Richard Goldstein
Division of Infection and Immunity
UCL
London WC1E 6BT

Abstract

Background: Viral population dynamics in long term viraemic antiretroviral therapy (ART) treated individuals have not been well characterised. Prolonged virologic failure on 2nd-line protease inhibitor (PI) based ART without emergence of major protease mutations is well recognised, providing an opportunity to study within-host evolution.

Methods: Using next-generation Illumina short read sequencing and in silico haplotype reconstruction we analysed whole genome sequences from longitudinal plasma samples of eight chronically infected HIV-1 individuals failing 2nd-line regimens from the ANRS 12249 TasP trial, in the absence of high frequency major PI resistance mutations. Plasma drug levels were measured by HPLC. Three participants were selective for in-depth variant and haplotype analyses, each with five or more timepoints spanning at least 16 months.

Results: During PI failure synonymous mutations were around twice as frequent as non-synonymous mutations across participants. Prior to or during exposure to PI, we observed several polymorphic amino acids in *gag* (e.g. T81A, T375N) which are have also been previously associated with exposure to protease inhibitor exposure. Although overall SNP frequency at abundance above 2% appeared stable across time in each individual, divergence from the consensus baseline sequence did increase over time. Non-synonymous changes were enriched in known polymorphic regions such as *env* whereas synonymous changes were more often observed to fluctuate in the conserved *pol* gene. Phylogenetic analyses of whole genome viral haplotypes demonstrated two common features: Firstly, evidence for selective sweeps following therapy switches or large changes in plasma drug concentrations, with hitchhiking of synonymous and non-synonymous mutations. Secondly, we observed competition between multiple viral haplotypes that intermingled phylogenetically alongside soft selective sweeps. The diversity of viral populations was maintained between successive timepoints with ongoing viremia, particularly in *env*. Changes in haplotype dominance were often distinct from the dynamics of drug resistance mutations in *reverse transcriptase* (RT), indicating the presence of softer selective sweeps and/or recombination.

Conclusions: Large fluctuations in variant frequencies with diversification occur during apparently 'stable' viremia on non-suppressive ART. Reconstructed haplotypes provided further evidence for sweeps during periods of partial adherence, and competition between haplotypes during periods of low drug exposure. Drug resistance mutations in RT can be used as markers of viral populations in the reservoir and we found evidence for loss of linkage disequilibrium for drug resistance mutations,

indicative of recombination. These data imply that even years of exposure to PIs, within the context of large stable populations displaying ongoing selective competition, may not precipitate emergence of major PI resistance mutations, indicating significant fitness costs for such mutations. Ongoing viral diversification within reservoirs may compromise the goal of sustained viral suppression.

78 **Introduction**

79 Even though HIV-1 infections are most commonly initiated with a single founder virus[1], acute and
80 chronic disease are characterised by extensive inter- and intra-participant genetic diversity[2,3]. The rate
81 and degree of diversification is influenced by multiple factors, including selection pressures imposed
82 by the adaptive immune system, exposure, and penetration of the virus to drugs, and tropism/fitness
83 constraints relating to replication and cell-to-cell transmission in different tissue compartments[4,5].
84 During HIV-1 infection, high rates of reverse transcriptase- (RT) related mutation and high viral
85 turnover during replication result in swarms of genetically diverse variants[6] which co-exist as
86 quasispecies. Existing literature on HIV-1 intrahost population dynamics is largely limited to untreated
87 infections, predominantly in subtype B infected individuals[2,7-9]. These works have shown non-linear
88 diversification of virus away from the founder strain during chronic untreated infection. Synonymous
89 mutations can be the product of neutral evolution, but they are also expected to occur more
90 commonly in established chronic infection due to higher fitness costs associated with non-
91 synonymous mutations[10], with the exception of immune escape during early infection[2].
92
93 Viral population dynamics in long-term viraemic antiretroviral therapy (ART) treated individuals have
94 not been well characterised. HIV rapidly accumulates drug-resistance associated mutations (DRMs),
95 particularly during non-suppressive first line ART[5,11]. As a result, ART-experienced participants failing
96 1st-line regimens for prolonged periods of time particularly in low- and middle-income countries
97 (LMICs), are characterised by high frequencies of common DRMs such as M184V, K65R and K103N[12].
98 By contrast, PI resistance mutations following failure of current boosted PI treatments are uncommon
99 in LMIC[13], a situation that differs for less potent drugs used in the early PI era[5]. A number of studies
100 have indicated that less well characterised mutations accumulating in the *gag* gene during PI failure
101 might also impact PI susceptibility[14-20], though common pathways have been difficult to discern, likely
102 reflecting plasticity to drug escape.
103
104 Prolonged virologic failure on PI regimens without emergence of protease mutations provides an
105 opportunity to study evolution under partially-suppressive ART. The process of selective sweeps in the
106 context of HIV-1 infection has previously been described[21,22] and it was reported that major PI DRMs
107 and other non-synonymous mutations in regulatory regions such as *pol,* significantly lower
108 fitness[2,23,24]. However, this has been typically shown outside of the context of longitudinal sampling.
109 By sampling participants consistently over several years, we propose that ongoing evolution is driven
110 by the dynamic flux between selection, recombination, and genetic drift.
111

112 We have deployed next-generation sequencing of stored blood plasma specimens from participants
113 in the Treatment as Prevention (TasP) ANRS 12249 study[25], conducted in Kwazulu-Natal, South Africa.
114 All participants were infected with HIV-1 subtype C and characterised as failing 2nd-line regimens
115 containing Lopinavir and Ritonavir (LPV/r), with prolonged virological failure in the absence of major
116 PI mutations[26]. In this paper, we report details of evolutionary dynamics during non-suppressive ART.
117

118 **Results**

119 *Participant Characteristics*

120 Eight participants with virological failure of 2nd-line PI based ART and at least two timepoints with
121 viraemia above 1000 copies/ml were selected from the French ANRS TasP trial for viral dynamic
122 analysis, including whole genome haplotye reconstruction (**Table 1**). Prior to participation in the TasP
123 trial, participants were accessing 1st-line regimens for an average of 5.6yrs (±2.7yrs). At baseline
124 enrolment visit into TasP (whilst failing 1st-line regimens), median viral load was 4.96×10^{10} (IQR:
125 4.17×10^{10} – 5.15×10^{10}); 12 DRMs were found at a threshold of >2%; the most common of which were
126 RT mutations K103N, M184V and P225H, consistent with previous use of d4T, NVP, EFV and FTC/3TC.
127 Six of the eight participants carried drug resistance mutations (DRMs) associated with PI failure at
128 minority frequencies (average 6.4%) and at usually at only single timepoints throughout the
129 longitudinal sampling. Observed mutations included L23I, I47V, M46I/L, G73S, V82A, N83D and I85V
130 (**Supplementary Tables 1a-3c**). Four of the six participants also carried major integrase stand inhibitor
131 (INSTI) mutations, again at minority frequencies (average 5.0%) and again normally only at single
132 timepoints (T97A, E138K, Y143H, Q148K).
133

134 *SNP frequencies and measures of diversity/divergence over time*

135 We used whole-genome sequencing (WGS) data to measure the frequencies of viral single nucleotide
136 polymorphisms (SNPs) relative to a dual-tropic subtype C reference sequence (AF411967) within
137 individuals over time using short-read deep-sequence data (**Figure 1**). We observed that SNPs
138 resulting from synonymous changes roughly mirrored those from non-synonymous changes, but the
139 former were two-to-three-fold more common. Furthermore, when we considered diversity relative to
140 the consensus sequence at baseline (switch from 1st- to 2nd-line regimens), we observed a moderate
141 decrease in diversity in four of the eight participants at the second timepoint, moderate increase in
142 diversity in one participant and relatively little diversity in the remaining three (**Figure 1,**
143 **Supplementary Figure 1**). From timepoint two onwards (all participants now on 2nd-line regimens for
144 >6 months), three participants saw increases in both synonymous and non-synonymous changes, two
145 participants saw decreases in those changes and three participants did not differ significantly. Finally,

146 HIV-1 subtype M group consensus sequences (Alignment ID: 102CG1) were downloaded from the Los
147 Alamos National Laboratory (LANL) and a merged consensus sequence was used as a proxy of a distant
148 ancestor for all participants. Using this ancestral sequence we measured sequence divergence over
149 sequential timepoints (**Figure 2**) to determine whether under non-suppressive ART, viral populations
150 were reverting towards an ancestral state, or diverging away from the M-group consensus. All but two
151 participants (15664 and 29447) showed a trend towards divergence away from the ancestor. This is
152 indicative of potential ongoing selection or could be due to random genetic drift. This finding contrasts
153 with studies in transmission where groups have demonstrated that transmitted viruses in the
154 'recipient' are closer to consensus as compared to the majority virus in the transmitting 'donor'[27].
155
156 To further investigate nucleotide diversity, we first considered all pairwise nucleotide distances of
157 each consensus WGS by timepoint and participant using a multidimensional scaling approach[28]. Intra-
158 participant nucleotide diversity varied considerably between participants (**Figure 3A-B**). Some
159 participants showed little diversity between timepoints (for example participant 16207), whereas
160 others showed higher diversity between timepoints (e.g. participant 22763). A similar range of
161 diversity profiles between participants were inferred by multidimensional scaling. Some participants
162 were tightly clustered, suggesting little change over time (**Figure 3a** participants 26892, 47939 &
163 16207), compared to others (participants 22828 & 28545).
164
165 When examining the *gag*, *pol* and *env* genes independently, the average diversity over all timepoints
166 (for participants 15664, 16207 and 22763) suggested that the highest diversity (**π**) was in the *env* gene.
167 Watterson's genetic diversity (**θ**) was highest in the *env* gene of participants 15664 and 16207. By
168 contrast, **θ** was highest in the *gag* gene for participant 22763 (**Table 2**).
169
170 *Phylogenetic analysis of inferred haplotypes*
171 The preceding diversity assessments suggested the existence of distinct viral haplotypes within each
172 participant. We therefore used a recently reported computational method[29] to infer 166 unique
173 haplotypes across all participants, with between 11 and 32 haplotypes (average 21) per participant
174 (**Figure 3C**). The number haplotypes changed dynamically between successive timepoints indicative
175 of dynamically shifting populations. To ensure that haplotypes were sensibly reconstructed, a
176 phylogeny of all consensus sequences was also inferred (**Supplementary Figure 2**). Three participants
177 were selected for deeper analysis based on these participants having the highest number of
178 longitudinal plasma samples. These included participants 15664, 16207 and 22763 who each had
179 whole-genome short-read deep-sequence data at more than five timepoints.

180

181 **Intra-host evolutionary dynamics and relation to drug levels**

182 Changing landscapes of non-synonymous and synonymous mutations

183 In the absence of major PI mutations, we first examined non-synonymous mutations across the whole
184 genome (**Figures 4-6**), with a specific focus on *pol* (to observe first and second line NRTI-associated
185 mutations) and *gag* (given its involvement in PI susceptibility). We and others have previously shown
186 that *gag* mutations accumulate during non-suppressive PI therapy[30,31]. There are also data suggesting
187 associations between *env* mutations and PI exposure[32,33]. **Supplementary Tables 1-3** summarise the
188 changes in variant frequencies of *gag*, *pol* and *env* mutations in participants over time. We found
189 between two and four mutations at sites previously associated with PI resistance in each participant,
190 all at persistently high frequencies (>90%) even in the absence of presumed drug pressure. This is
191 explained by the fact that a significant proportion of sites associated with PI exposure are also
192 polymorphic across HIV-1 subtypes[18,34]. To complement this analysis, we examined underlying
193 synonymous mutations across the genome. This revealed complex changes in the frequencies of
194 multiple nucleotide residues across all genes. These changes often formed distinct 'chevron-like'
195 pattens between timepoints (**Figures 4c & 5b**), indicative of linked alleles dynamically shifting and
196 suggestive of competition between viral haplotypes.

197

198 **Participant 15664** had consistently low drug plasma concentration of all drugs at each measured
199 timepoint, with detectable levels measured only at month 15 and beyond (**Figure 4a**). At baseline,
200 whilst on NNRTI-based 1st-line ART, known NRTI (M184V) and NNRTI (K103N and P225H) DRMs[5] were
201 at high prevalence in the virus populations which is as expected whilst adhering to 1st-line treatments.
202 Haplotype reconstruction and subsequent analysis inferred the presence of a majority haplotype
203 carrying all three of these mutations at baseline, as well as a minority haplotype with none of the RT
204 mutations (**Figure 4d**, orange circles). Following the switch to a 2nd-line regimen, variant frequencies
205 of M184V and P225H dropped below detection limits (<2% of reads), whilst K103N remained at high
206 frequency (**Figure 4b**). Haplotype analysis was concordant, revealing that viruses with K103N, M184V
207 and P225H were replaced by haplotypes with only K103N (**Figure 4d**, large brown circles), with
208 minority haplotypes that had no RT mutations (**Figure 4d**, small brown circles). At timepoint two
209 (month 8), there were also numerous synonymous mutations observed at high frequency in both *gag*
210 and *pol* genes, corresponding with the switch to a 2nd-line regimen. At timepoint three (15 months
211 post-switch to 2nd-line regimen) drug concentrations were highest, though still low in absolute terms,
212 indicating partial adherence. Between timepoints three and four we observed a two-log reduction in
213 viral load, with modest change in frequency of RT DRMs. However, we observed synonymous variant

214 frequency shifts predominantly in both *gag* and *pol* genes, as indicated by multiple variants increasing
215 and decreasing contemporaneously, creating characteristic chevron patterning (**Figure 4b**). However
216 many of the changes were between intermediate frequencies, (e.g. between 20% and 60%), which
217 differed from changes between time points one and two where multiple variants changed more
218 dramatically in frequency from <5% to more than 80%, indicating harder selective sweep. These data
219 are in keeping with a soft selective sweep between time points 3 and 5. Between time points five and
220 six, the final two samples, there was another population shift - M184V and P225H frequencies fell
221 below the detection limit at timepoint six, whereas the frequency of K103N dropped from almost
222 100% to around 75% (**Figure 4b**). This was consistent with haplotype reconstruction, which inferred a
223 dominant viral haplotype at timepoint six bearing only K103N, as well as a minor haplotype with no
224 DRMs at all (**Figure 2d**, pink circles). The inferred haplotype without DRMs was nonetheless
225 phylogenetically distinct from the timepoint one minority haplotype (**Figure 4d**, compare small orange
226 and pink circles in upper clade).
227
228 Upon examining the phylogenetic relationships of the inferred haplotype sequences, there were two
229 distinct clades with members of both clades present at all time points apart from the first. This
230 suggests an intermingling of viral haplotypes and competition. DRMs showed some segregation by
231 clade; viruses carrying a higher frequency of DRMs were observed in the lower clade (Clade B, **Figure**
232 **4d**), and those with either K103N alone, or no DRMs were preferentially located in the upper clade
233 (Clade A, **Figure 4d**). However, this relationship was not clear cut, and therefore consistent with
234 competition between haplotypes during low drug exposure. Soft sweeps were evident, given the
235 increasing diversity (**Figure 1**) of this participant, as well as constrained variant frequencies between
236 20-80% (**Figure 4b,c**).
237
238 **Participant 16207.** Viral load in this participant were consistently elevated >10,000 copies/ml (**Figure**
239 **5a)**. As with participant 15664, drug concentrations in blood plasma remained extremely low or absent
240 at each measured timepoint, consistent with non-adherence to the prescribed regimen. There was
241 almost no change in the frequency of DRMs throughout the follow up period, even when making the
242 switch to the 2nd-line regimen. NNRTI resistance mutations such as K103N are known to have minimal
243 fitness costs[24] and can therefore persist in the absence of NNRTI pressure. Throughout treatment the
244 participant maintained K103N at a frequency of >95% but also carried several integrase strand transfer
245 inhibitor (INSTI) associated changes (E157Q) and PI-exposure associated amino acid replacements
246 (L23I and M46I) at low frequencies at timepoints two and three. Despite little change in DRM site
247 frequencies, very significant viral population shifts were observed at the whole genome level, again

248 indicative of selective sweeps (**Figures 5b-c**). Between timepoints one and four, several linked
249 mutations changed abundance contemporaneously, generating chevron-like patterns of non-
250 synonymous changes in *env* specifically (blue lines). A large number of alleles increased in frequency
251 from <20% to >80% at the same time as numerous others decreased in frequency from above 80% to
252 below 20%. Whereas large shifts in gag and pol alleles also occurred, the mutations involved were
253 almost exclusively synonymous (red and green lines). These putative selective sweeps in *env* were
254 evident in the phylogenetic analysis (**Figure 5d**, see long branch lengths between timepoints one and
255 four, and cladal structure) possibly driven by neutralising antibodies and/or T-cell immune pressures.
256
257 Phylogenetic analysis of inferred whole genome haplotypes overall showed a distinct cladal structure
258 as observed in 15664 (**Figure 5d**), although the dominant haplotypes were mostly observed in the
259 lower clade (Clade B, **Figure 5d**). K103N, the only major DRM, was inferred in both clades A and B.
260 Haplotypes did not cluster by time point. Significant diversity in haplotypes from this participant was
261 confirmed by MDS (**Supplementary Figure 3**).
262
263 **Participant 22763** was notable for a number of large shifts in variant frequencies across multiple drug
264 resistance associated residues and synonymous sites. Drug plasma concentration for different drugs
265 was variable yet detectable at most measured timepoints reflecting changing levels of adherence
266 across the treatment period (**Figure 6a).** Non-PI DRMs such as M184V, P225H and K103N were present
267 at baseline (time of switch from first to second line treatments). These mutations persisted despite
268 synonymous changes between time points one and two. Most of the highly variable synonymous
269 changes in this participant were found in the *gag* and *pol* genes (as in participant 16207) (**Figure 6c**),
270 but in this case *env* displayed large fluctuations in synonymous and non-synonymous allelic
271 frequencies over time. At timepoint three therapeutic concentrations of LPV/r and TDF were
272 measured in plasma and haplotypes clustered separately from the first two timepoints (**Figure 6d**,
273 green circles). NGS confirmed that the D67N, K219Q, K65R, L70R, M184V DRMs and NNRTI-resistance
274 mutations were present at low frequencies from timepoint three onwards. Of note, between
275 timepoints three and six, therapeutic concentration of tenofovir (TDF) was detectable, and coincided
276 with increased frequencies of the canonical TDF DRM, K65R[5]. The viruses carrying K65R outcompeted
277 those carrying the thymidine analogue mutants (TAMs) D67N and K70R, whilst the lamivudine (3TC)
278 associated resistance mutation, M184V, persisted throughout. In the final three timepoints M46I
279 emerged in *protease*, but never increased in frequency above <6%. At timepoint seven, populations
280 shifted again with some haplotypes resembling those previously timepoint four, with D67N and K70R
281 again being predominant over K65R in *reverse transcriptase* (**Figure 6d**, green and blue circles). At the

282 final timepoint (eight) the frequency of K103N was approximately 85% and the TAM-bearing
283 populations continued to dominate over the K65R population, which at this timepoint had a low
284 frequency.
285
286 Although the DRM profile suggested the possibility of a selective sweep, we did not observe groups
287 of other non-synonymous or synonymous alleles exhibiting dramatic frequency shifts, i.e. we did not
288 observe the same 'chevron patterns' in synonymous- and non-synonymous variant plots (**Figure 6b-**
289 **c**) as those seen in participants 15664 and 16207. Indeed, haplotypes were spread throughout the
290 phylogenetic tree, consistent with low drug pressure. Some inferred haplotypes had K65R and others
291 the TAMs D67N and K70R. K65R was not observed in combination with D67N or K70R, consistent with
292 previously reported antagonism between K65R and TAMs whereby these mutations are not
293 commonly found together within a single genome[35-37]. One possible explanation for the disconnect
294 between the trajectories of DRM frequencies over time and haplotype phylogeny is recombination.
295 Alternatively, emergence of haplotypes from previously unsampled reservoir with different DRM
296 profile is possible, but one might have expected other mutations to characterise such haplotypes that
297 would manifest as change in frequencies of large numbers of other mutations.
298
299 **Discussion**
300 The proportion of people living with HIV (PLWH) accessing ART has increased from 24% in 2010, to
301 68% in 2020[38,39]. However, with the scale-up of ART, there has also been an increase in both pre-
302 treatment drug resistance (PDR)[40,41] and acquired drug resistance[12,42] to 1st-line ART regimens
303 containing NNRTIs. Integrase inhibitors (specifically dolutegravir) are now recommended for first-line
304 regimens by the WHO in regions where PDR exceeds 10%[43]. Boosted PI-containing regimens remain
305 second line drugs following first 1st-line failure, though one unanswered question relates to the nature
306 of viral populations during failure on PI-based ART where major mutations in *protease*, described
307 largely for less potent PI, have not emerged. Here we have comprehensively analysed viral populations
308 present in longitudinally collected plasma samples of chronically-infected HIV-1 participants under
309 non-suppressive 2nd-line ART.
310
311 With the vast majority of PLWH treated in the post-ART era, virus dynamics during non-suppressive
312 ART is important to understand, as there may be implications for future therapeutic success. For
313 example broadly neutralising antibodies (bNab) are being tested not only for prevention, but also as
314 part of remission strategies in combination with latency reversal agents. We know that HIV sensitivity

315 to bNab is dependent on *env* diversity[44,45], and therefore prolonged ART failure with viral
316 diversification could compromise sensitivity to these agents.
317
318 Our understanding of virus dynamics largely stems from studies that were limited to untreated
319 individuals[46], with largely subgenomic data analysed rather than whole genome[9]. Traditional analysis
320 of quasispecies distribution, for example as reported by Yu et al[47], suggests that the viral diversity
321 increases in longitudinal samples. However the findings of Yu et al were based entirely on short-read
322 NGS data without considering whole-genome haplotypes. The added benefit of examining whole
323 genome is that linked mutations can be identified statistically using an approach that we gave recently
324 developed[29]. Indeed haplotype reconstruction has proved beneficial in the analysis of
325 compartmentalisation and diversification of several RNA viruses, including HIV-1, CMV and SARS-CoV-
326 2[30,48,49].
327
328 Key findings of this study were: firstly that diversity increased over time with variable trajectory away
329 from the consensus baseline sequence and also the reconstructed ancestral subtype M consensus.
330 Approximately half of the participants appeared to diversify away from the reconstructed ancestral
331 subtype M sequence, but interestingly three participants showed possible diversification back
332 towards the ancestral consensus (albeit with insufficient statistical support).
333
334 Secondly, and in contrast to the fractions of synonymous and non-synonymous mutations reported
335 by Zanini et al in a longitudinal untreated dataset[2], we show that the fractions of synonymous
336 mutations are generally two-to-three fold higher than non-synonymous mutations during non-
337 suppressive ART in chronic infection. This finding may reflect early versus chronic infection and
338 differing selective pressures. Haplotype reconstruction revealed evidence for competing haplotypes,
339 with evidence for numerous soft selective sweeps in phylogenies, evidenced by intermingling of
340 haplotypes during periods where there was low drug concentration measured in participant's blood
341 plasma.
342
343 Individuals in the present study were treated with Ritonavir boosted Lopinavir along with two NRTIs
344 (typically Tenofovir + Emtricitabine). We observed significant change in the frequencies of NRTI
345 mutations in two of the three participants studied in-depth. These fluctuations likely reflected
346 adherence to the 2nd-line regimen though we saw evidence for possible archived virus populations
347 with DRMs emerging during follow-up because large changes in DRM frequency were not always
348 accompanied by changes at other sites. This is consistent with soft sweeps occurring and that non-

349 DRMs do not necessarily drift with other mutations to fixation[21] and that the same mutations are
350 occurring on different backgrounds. As frequencies of RT DRMs did not always segregate with
351 haplotype frequencies, we suggest that a high number of recombination events, known to be common
352 in HIV infections, was responsible for the haplotypic diversity.
353
354 Although no participant developed major DRMS at consistently high frequencies to PIs
355 (https://hivdb.stanford.edu/dr-summary/resistance-notes/PI/), we did observe non-synonymous
356 mutations associated with PI exposure that are also known to be polymorphic; however, there was no
357 temporal evidence of specific changes being associated with selective sweeps. For example PI
358 exposure associated residues in matrix (positions 76 and 81) were observed in participant 16207 prior
359 to PI initiation[50]. Furthermore, participant 16207 was one of few participants who achieved two
360 partial suppressions (<750 copies/ml). After both of these partial suppressions, the rebound
361 populations appeared to be less diverse, consistent with drug-resistant virus re-emerging.
362
363 Mutations in all genes that are further apart than 100bp are subject to shuffling via recombination[51].
364 Indeed, particularly in participant 22763, there is evidence of recombination between timepoint
365 corresponding to months 10 and 27. Whilst we did not undertake a formal recombination analysis at
366 this time, in the future insights into the relationship between DRMs and the dissociation from
367 synonymous changes, relative to genomic regions that have been transferred by recombination, may
368 lead to additional insights of viral populations pressures under non-suppressive ART.
369
370 This study had some limitations – we examined in-detail three participants with ongoing viraemia and
371 variable adherence to 2nd-line drug regimens. Despite the small sample size, this type of longitudinal
372 sampling of ART-experienced participants in unprecedented. We are confident that the combination
373 of computational analyses has provided a detailed understanding of viral dynamics under non-
374 suppressive ART and is directly applicable to wider datasets. The method used to reconstruct viral
375 haplotypes *in silico* is novel and has previously been validated in HIV-positive participants with CMV[48].
376 Validation of haplotypes is based on inputting a known mix of artificial viruses and comparing the
377 output to the known input, as is common with such software. We are confident that approach
378 implemented by HaROLD has accurately, if conservatively estimated haplotype frequencies and future
379 studies should look to validate these frequencies using an *in vitro* method such as single genome
380 amplification. Despite there being high viral loads present at each of the analysed timepoints, nuances
381 of the sequencing method led in some cases to suboptimal degrees of gene coverage (**Supplementary**
382 **Figure 4**). Mapping metrics showed that gaps in sequence coverage were random, which excludes the

383 possibility of systematic bias in the participant data. To ensure that uneven sequencing coverage did
384 not bias our analyses, we ensured that variant analysis was only performed where coverage was >10
385 reads.
386
387 In summary we have found compelling evidence of HIV-1 within host viral diversification and
388 haplotype competition during non-suppressive ART, in addition to recombination. Going forward,
389 participants failing PI-based regimens are likely to be switched to INSTI-based ART (specifically
390 Dolutegravir in South Africa) prior to genotypic typing or resistance analysis. Although the prevalence
391 of underlying major INSTI resistance mutations is low in sub-Saharan Africa[52,53], this approach needs
392 assessment given data linking individuals with NNRTI resistance with poorer virological outcomes on
393 Dolutegravir[54], coupled with a history of intermittent adherence. The increases in diversity generated
394 during long term PI failure may have biological effects that renders durable suppression less likely.
395
396 **Methods**
397 *Study & Participant selection*
398 This cohort was nested within the French ANRS 12249 Treatment as Prevention (TasP) trial[25]. TasP was
399 a cluster-randomised trial comparing an intervention arm who offered ART after HIV diagnosis
400 irrespective of participant CD4 + count, to a control arm which offered ART according to prevailing
401 South African guidelines. A subset of 44 longitudinal samples from 8 chronically infected participants.
402 Participants were selected for examination if there were >3 timepoint samples available. All samples
403 were collected from blood plasma. The Illumina MiSeq platform was used and an adapted protocol
404 for sequencing[55]. Adherence to 2nd-line regimens was measured by HPLC using plasma concentration
405 of drug levels as a proxy. Drug levels were measured at each timepoint with detectable viral loads,
406 post-PI initiation.
407
408 Ethical approval was originally grant by the Biomedical Research Ethics Committee (BFC 104/11) at
409 the University of KwaZulu-Natal, and the Medicines Control Council of South Africa for the TasP trial
410 (Clinicaltrials.gov: NCT01509508; South African Trial Register: DOH-27-0512-3974). The study was also
411 authorized by the KwaZulu-Natal Department of Health in South Africa. Written informed consent was
412 obtained from all participants. Original ethical approval also included downstream sequencing of
413 blood plasma samples and analysis of those sequences to better understand drug resistance. No
414 additional ethical approval was required for this.
415
416 Illumina Sequencing

417 Sequencing of viral RNA was performed as previously described by Derache et al[56] using a modified
418 protocol previously described by Gall et al[57]. Briefly, RNA was extracted from 1ml of plasma with
419 detectable viral load of >1000 copies/ml, using QIAamp Viral RNA mini kits (Qiagen, Hilden, Germany),
420 and eluted in 60µl of elution buffer. The near-full HIV genome was amplified with 4 subtype C primers
421 pairs, generating 4 overlapping amplicons of between 2100 and 3900kb.
422
423 DNA concentrations of amplicons were quantified with the Qubit dsDNA HS Assay kit (Invitrogen,
424 Carlsbad, CA). Diluted amplicons were pooled equimolarly and prepared for library using the Nextera
425 XT DNA Library preparation and the Nextera XT DNA sample preparation index kits (Illumina, San
426 Diego, CA), following the manufacturer's protocol.
427
428 *Genomics & Bioinformatics*
429 Poor quality reads (with Phred score <30) and adapter sequences were trimmed from FastQ files with
430 TrimGalore! v0.6.519[58] and mapped to a clade C South African reference genome (AF411967.1) with
431 BWA-MEM[59]. The reference genome was manually annotated in Geneious Prime v2020.3 with DRMs
432 according to the Stanford HivDB[60]. Optical PCR duplicate reads were removed using Picard tools
433 (http://broadinstitute.github.io/picard). Finally, QualiMap2[61] was used to assess the mean mapping
434 quality scores and coverage in relation to the reference genome for the purpose of excluding poorly
435 mapped sequences from further analysis. Single nucleotides polymorphisms (SNPs) were called using
436 VarScan2[62] with a minimum average quality of 20, minimum variant frequency of 2% and in at least
437 10 reads. These were then annotated by gene, codon and amino acid alterations using an in-house
438 script[63] modified to utilise HIV genomes.
439
440 All synonymous variants and DRMs were examined, and their frequency compared across successive
441 timepoints. Synonymous variants were excluded from analysis if their prevalence remained at ≤10%
442 or ≥90% across all timepoints. DRMs were retained for analysis if they were present at over 2%
443 frequency and on at least two reads. A threshold of 2% is supported by a study evaluating different
444 analysis pipelines, which reported fewer discordances over this cut-off[64].
445
446 *Haplotype Reconstruction & Phylogenetics*
447 Whole-genome viral haplotypes were constructed for each participant timepoint using Haplotype
448 Reconstruction for Longitudinal Samples (HaROLD)[65]. Briefly, SNPs were assigned to each haplotype
449 such that the frequency of variants was equal to the sum of the frequencies of haplotypes containing
450 a specific variant. Maximal log likelihood was used to optimise time-dependent frequencies for

longitudinal haplotypes which was calculated by summing over all possible assignment of haplotype variants. Haplotypes were then constructed based on posterior probabilities. After constructing haplotypes, a refinement process remapped reads from BAM files to those constructed haplotypes. The number of haplotypes either increased or decreased as a result of combination or division according to AIC scores, in order to present the most accurate representation of viral populations at each timepoint.

Whole-genome nucleotide diversity was calculated from BAM files using an in-house script (https://github.com/ucl-pathgenomics/NucleotideDiversity). Briefly diversity is calculated by fitting all observed variant frequencies to either a beta distribution or four-dimensional Dirichlet distribution plus delta function (representing invariant sites). These parameters were optimised by maximum log likelihood. Individual gene nucleotide diversity (π), number of segregating sites (S) and Watterson's genetic diversity (θ) were calculated separately using all reconstructed haplotypes per participant, using DnaSP v6.12.03[66].

Maximum-likelihood phylogenetic trees and ancestral reconstruction were performed using IQTree2 v2.1.2[67]. Evolutionary model selection for trees were inferred using ModelFinder[68] and trees were estimated using the GTR+F+I model with 1000 ultrafast bootstrap replicates[69]. All trees were visualised with Figtree v.1.4.4 (http://tree. bio.ed.ac.uk/software/figtree/), rooted on the AF411967.1 reference sequence, and nodes arranged in descending order. Phylogenies were manipulated and annotated using ggtrree v2.24.

Multi Dimension Scaling (MDS) Plots

Whole genomes were obtained as previously described. Pairwise distances between these consensus sequences were calculated using the dist.dna() package in R, with a TN93 nucleotide-nucleotide substitution matrix[70] and with pairwise deletion by way of the R package Ape v.5.4[71]. Multi-dimensional scaling (MDS) was implemented using the cmdscale() function with pairwise deletion in R v4.0.4. Much like PCA is a method to attempt to simplify complex data into a more interpretable format, by reducing dimensionality of data whilst retaining most of the variation. In a genomics context we can use this on pairwise distance matrices, where each dimension is a sequence with data points of n-1 sequences pairwise distance. The process was repeated with whole genome haplotype sequences.

Funding

SAK is supported by the Bill and Melinda Gates Foundation: OPP1175094. RKG is supported by Wellcome Trust Senior Fellowship in Clinical Science: WT108082AIA.

Transparency declarations

RKG has received ad hoc consulting fees from Gilead, ViiV and UMOVIS Lab.

References

1 Abrahams, M. R. *et al.* Quantitating the multiplicity of infection with human immunodeficiency virus type 1 subtype C reveals a non-poisson distribution of transmitted variants. *J Virol* **83**, 3556-3567, doi:10.1128/JVI.02132-08 (2009).

2 Zanini, F., Puller, V., Brodin, J., Albert, J. & Neher, R. A. In vivo mutation rates and the landscape of fitness costs of HIV-1. *Virus Evol* **3**, vex003, doi:10.1093/ve/vex003 (2017).

3 Salemi, M. The intra-host evolutionary and population dynamics of human immunodeficiency virus type 1: a phylogenetic perspective. *Infect Dis Rep* **5**, e3-e3, doi:10.4081/idr.2013.s1.e3 (2013).

4 Lemey, P., Rambaut, A. & Pybus, O. G. HIV evolutionary dynamics within and among hosts. *Aids Reviews* **8**, 125-140 (2006).

5 Collier, D. A., Monit, C. & Gupta, R. K. The Impact of HIV-1 Drug Escape on the Global Treatment Landscape. *Cell host & microbe* **26**, 48-60, doi:10.1016/j.chom.2019.06.010 (2019).

6 Biebricher, C. K. & Eigen, M. What is a quasispecies? *Curr Top Microbiol Immunol* **299**, 1-31, doi:10.1007/3-540-26397-7_1 (2006).

7 Lythgoe, K. A. & Fraser, C. New insights into the evolutionary rate of HIV-1 at the within-host and epidemiological levels. *Proceedings of the Royal Society B: Biological Sciences* **279**, 3367-3375 (2012).

8 Hedskog, C. *et al.* Dynamics of HIV-1 quasispecies during antiviral treatment dissected using ultra-deep pyrosequencing. *PloS one* **5**, e11345 (2010).

9 Shankarappa, R. *et al.* Consistent viral evolutionary changes associated with the progression of human immunodeficiency virus type 1 infection. *Journal of virology* **73**, 10489-10502 (1999).

10 Theys, K. *et al.* Within-patient mutation frequencies reveal fitness costs of CpG dinucleotides and drastic amino acid changes in HIV. *PLoS genetics* **14**, e1007420, doi:10.1371/journal.pgen.1007420 (2018).

518 11 Masikini, P. & Mpondo, B. C. HIV drug resistance mutations following poor adherence in HIV-
519 infected patient: a case report. *Clin Case Rep* **3**, 353-356, doi:10.1002/ccr3.254 (2015).
520 12 TenoRes Study, G. Global epidemiology of drug resistance after failure of WHO
521 recommended first-line regimens for adult HIV-1 infection: a multicentre retrospective
522 cohort study. *Lancet Infect Dis* **16**, 565-575, doi:10.1016/S1473-3099(15)00536-8 (2016).
523 13 Collier, D. *et al.* Virological Outcomes of Second-line Protease Inhibitor-Based Treatment for
524 Human Immunodeficiency Virus Type 1 in a High-Prevalence Rural South African Setting: A
525 Competing-Risks Prospective Cohort Analysis. *Clinical infectious diseases : an official*
526 *publication of the Infectious Diseases Society of America* **64**, 1006-1016,
527 doi:10.1093/cid/cix015 (2017).
528 14 Giandhari, J. *et al.* Genetic Changes in HIV-1 Gag-Protease Associated with Protease
529 Inhibitor-Based Therapy Failure in Pediatric Patients. *AIDS Res Hum Retroviruses* **31**, 776-
530 782, doi:10.1089/AID.2014.0349 (2015).
531 15 Kelly Pillay, S., Singh, U., Singh, A., Gordon, M. & Ndungu, T. Gag drug resistance mutations
532 in HIV-1 subtype C patients, failing a protease inhibitor inclusive treatment regimen, with
533 detectable lopinavir levels. *Journal of the International AIDS Society* **17**, 19784 (2014).
534 16 Sutherland, K. A. *et al.* Evidence for Reduced Drug Susceptibility without Emergence of
535 Major Protease Mutations following Protease Inhibitor Monotherapy Failure in the SARA
536 Trial. *PloS one* **10**, e0137834, doi:10.1371/journal.pone.0137834 (2015).
537 17 Sutherland, K. A. *et al.* Phenotypic characterization of virological failure following
538 lopinavir/ritonavir monotherapy using full-length Gag-protease genes. *The Journal of*
539 *antimicrobial chemotherapy* **69**, 3340-3348, doi:10.1093/jac/dku296 (2014).
540 18 Sutherland, K. A. *et al.* Gag-Protease Sequence Evolution Following Protease Inhibitor
541 Monotherapy Treatment Failure in HIV-1 Viruses Circulating in East Africa. *AIDS research and*
542 *human retroviruses* **31**, 1032-1037, doi:10.1089/aid.2015.0138 (2015).
543 19 Day, C. L. *et al.* Proliferative capacity of epitope-specific CD8 T-cell responses is inversely
544 related to viral load in chronic human immunodeficiency virus type 1 infection. *Journal of*
545 *virology* **81**, 434-438, doi:10.1128/JVI.01754-06 (2007).
546 20 Blanch-Lombarte, O. *et al.* HIV-1 Gag mutations alone are sufficient to reduce darunavir
547 susceptibility during virological failure to boosted PI therapy. *The Journal of antimicrobial*
548 *chemotherapy* **75**, 2535-2546, doi:10.1093/jac/dkaa228 (2020).
549 21 Feder, A. F. *et al.* More effective drugs lead to harder selective sweeps in the evolution of
550 drug resistance in HIV-1. *Elife* **5**, e10670, doi:10.7554/eLife.10670 (2016).

551 22 Harris, R. B., Sackman, A. & Jensen, J. D. On the unfounded enthusiasm for soft selective
552 sweeps II: Examining recent evidence from humans, flies, and viruses. *PLoS genetics* **14**,
553 e1007859 (2018).
554 23 Dam, E. *et al.* Gag mutations strongly contribute to HIV-1 resistance to protease inhibitors in
555 highly drug-experienced patients besides compensating for fitness loss. *PLoS pathogens* **5**,
556 e1000345 (2009).
557 24 Cong, M.-e., Heneine, W. & García-Lerma, J. G. The fitness cost of mutations associated with
558 human immunodeficiency virus type 1 drug resistance is modulated by mutational
559 interactions. *Journal of virology* **81**, 3037-3041 (2007).
560 25 Iwuji, C. C. *et al.* Evaluation of the impact of immediate versus WHO recommendations-
561 guided antiretroviral therapy initiation on HIV incidence: the ANRS 12249 TasP (Treatment
562 as Prevention) trial in Hlabisa sub-district, KwaZulu-Natal, South Africa: study protocol for a
563 cluster randomised controlled trial. *Trials* **14**, 230, doi:10.1186/1745-6215-14-230 (2013).
564 26 Organization, W. H. *Consolidated guidelines on the use of antiretroviral drugs for treating*
565 *and preventing HIV infection: recommendations for a public health approach*. (World Health
566 Organization, 2016).
567 27 Carlson, J. M. *et al.* Selection bias at the heterosexual HIV-1 transmission bottleneck. *Science*
568 **345**, 1254031, doi:10.1126/science.1254031 (2014).
569 28 Cox, M. A. & Cox, T. F. in *Handbook of data visualization* 315-347 (Springer, 2008).
570 29 Pang, J. *et al.* Haplotype assignment of longitudinal viral deep-sequencing data using co-
571 variation of variant frequencies. *bioRxiv*, 444877, doi:10.1101/444877 (2020).
572 30 Datir, R. *et al.* In Vivo Emergence of a Novel Protease Inhibitor Resistance Signature in HIV-1
573 Matrix. *mBio* **11**, e02036-02020, doi:10.1128/mBio.02036-20 (2020).
574 31 Kletenkov, K. *et al.* Role of Gag mutations in PI resistance in the Swiss HIV cohort study:
575 bystanders or contributors? *Journal of Antimicrobial Chemotherapy* **72**, 866-875,
576 doi:10.1093/jac/dkw493 (2016).
577 32 Rabi, S. A. *et al.* Multi-step inhibition explains HIV-1 protease inhibitor pharmacodynamics
578 and resistance. *The Journal of clinical investigation* **123**, 3848-3860, doi:10.1172/JCI67399
579 (2013).
580 33 Manasa, J. *et al.* Evolution of gag and gp41 in Patients Receiving Ritonavir-Boosted Protease
581 Inhibitors. *Sci Rep* **7**, 11559, doi:10.1038/s41598-017-11893-8 (2017).
582 34 Datir, R., El Bouzidi, K., Dakum, P., Ndembi, N. & Gupta, R. K. Baseline PI susceptibility by
583 HIV-1 Gag-protease phenotyping and subsequent virological suppression with PI-based

584 second-line ART in Nigeria. *The Journal of antimicrobial chemotherapy* **74**, 1402-1407,
585 doi:10.1093/jac/dkz005 (2019).
586 35 Parikh, U. M., Zelina, S., Sluis-Cremer, N. & Mellors, J. W. Molecular mechanisms of
587 bidirectional antagonism between K65R and thymidine analog mutations in HIV-1 reverse
588 transcriptase. *Aids* **21**, 1405-1414 (2007).
589 36 Parikh, U. M., Bacheler, L., Koontz, D. & Mellors, J. W. The K65R mutation in human
590 immunodeficiency virus type 1 reverse transcriptase exhibits bidirectional phenotypic
591 antagonism with thymidine analog mutations. *Journal of virology* **80**, 4971-4977 (2006).
592 37 Parikh, U. M., Barnas, D. C., Faruki, H. & Mellors, J. W. Antagonism between the HIV-1
593 reverse-transcriptase mutation K65R and thymidine-analogue mutations at the genomic
594 level. *The Journal of infectious diseases* **194**, 651-660 (2006).
595 38 Department of Health. 2019 ART Clinical Guidelines for the Management of HIV in Adults,
596 Pregnancy, Adolescents, Children, Infants and Neonates. (Republic of South Africa National
597 Department of Health, 2019).
598 39 UNAIDS. *Global HIV & AIDS statistics — 2020 fact sheet*,
599 <https://www.unaids.org/en/resources/fact-sheet> (2020), Accessed 3rd March 2021.
600 40 Gupta, R. K. *et al.* HIV-1 drug resistance before initiation or re-initiation of first-line
601 antiretroviral therapy in low-income and middle-income countries: a systematic review and
602 meta-regression analysis. *Lancet Infect Dis* **18**, 346-355, doi:10.1016/S1473-3099(17)30702-
603 8 (2018).
604 41 Gupta, R. K. *et al.* Global trends in antiretroviral resistance in treatment-naive individuals
605 with HIV after rollout of antiretroviral treatment in resource-limited settings: a global
606 collaborative study and meta-regression analysis. *Lancet* **380**, 1250-1258,
607 doi:10.1016/S0140-6736(12)61038-1 (2012).
608 42 Gregson, J. *et al.* Occult HIV-1 drug resistance to thymidine analogues following failure of
609 first-line tenofovir combined with a cytosine analogue and nevirapine or efavirenz in sub
610 Saharan Africa: a retrospective multi-centre cohort study. *Lancet Infect Dis*,
611 doi:10.1016/S1473-3099(16)30469-8 (2017).
612 43 WHO, C. Global Fund. HIV drug resistance report. 2017. *World Health Organisation* (2017).
613 44 Stefic, K., Bouvin-Pley, M., Braibant, M. & Barin, F. Impact of HIV-1 diversity on its sensitivity
614 to neutralization. *Vaccines* **7**, 74 (2019).
615 45 Pancera, M. *et al.* Structure and immune recognition of trimeric pre-fusion HIV-1 Env.
616 *Nature* **514**, 455-461 (2014).

617 46 Shankarappa, R. *et al.* Consistent viral evolutionary changes associated with the progression
618 of human immunodeficiency virus type 1 infection. *Journal of virology* **73**, 10489-10502,
619 doi:10.1128/JVI.73.12.10489-10502.1999 (1999).
620 47 Yu, F. J. *et al.* The Transmission and Evolution of HIV-1 Quasispecies within One Couple: a
621 Follow-up Study based on Next-Generation Sequencing. *Scientific reports* **8**, 1-8, doi:ARTN
622 140410.1038/s41598-018-19783-3 (2018).
623 48 Pang, J. *et al.* Mixed cytomegalovirus genotypes in HIV-positive mothers show
624 compartmentalization and distinct patterns of transmission to infants. *Elife* **9**, e63199,
625 doi:10.7554/eLife.63199 (2020).
626 49 Boshier, F. A. T. *et al.* Remdesivir induced viral RNA and subgenomic RNA suppression, and
627 evolution of viral variants in SARS-CoV-2 infected patients. *medRxiv*,
628 2020.2011.2018.20230599, doi:10.1101/2020.11.18.20230599 (2020).
629 50 Parry, C. M. *et al.* Three residues in HIV-1 matrix contribute to protease inhibitor
630 susceptibility and replication capacity. *Antimicrobial agents and chemotherapy* **55**, 1106-
631 1113, doi:10.1128/AAC.01228-10 (2011).
632 51 Neher, R. A. & Leitner, T. Recombination rate and selection strength in HIV intra-patient
633 evolution. *PLoS Comput Biol* **6**, e1000660 (2010).
634 52 El Bouzidi, K. *et al.* High prevalence of integrase mutation L74I in West African HIV-1
635 subtypes prior to integrase inhibitor treatment. *J Antimicrob Chemother* **75**, 1575-1579,
636 doi:10.1093/jac/dkaa033 (2020).
637 53 Derache, A. *et al.* Predicted antiviral activity of tenofovir versus abacavir in combination with
638 a cytosine analogue and the integrase inhibitor dolutegravir in HIV-1-infected South African
639 patients initiating or failing first-line ART. *The Journal of antimicrobial chemotherapy*,
640 doi:10.1093/jac/dky428 (2018).
641 54 Siedner, M. J. *et al.* Reduced efficacy of HIV-1 integrase inhibitors in patients with drug
642 resistance mutations in reverse transcriptase. *Nat Commun* **11**, 5922, doi:10.1038/s41467-
643 020-19801-x (2020).
644 55 Iwuji, C. *et al.* Universal test and treat is not associated with sub-optimal antiretroviral
645 therapy adherence in rural South Africa: the ANRS 12249 TasP trial. *J Int AIDS Soc* **21**,
646 e25112, doi:10.1002/jia2.25112 (2018).
647 56 Derache, A. *et al.* Impact of Next-generation Sequencing Defined Human Immunodeficiency
648 Virus Pretreatment Drug Resistance on Virological Outcomes in the ANRS 12249 Treatment-
649 as-Prevention Trial. *Clinical infectious diseases : an official publication of the Infectious*
650 *Diseases Society of America* **69**, 207-214, doi:10.1093/cid/ciy881 (2019).

651 57 Gall, A. *et al.* Universal amplification, next-generation sequencing, and assembly of HIV-1
652 genomes. *Journal of clinical microbiology* **50**, 3838-3844, doi:10.1128/JCM.01516-12 (2012).
653 58 Martin, M. J. E. j. Cutadapt removes adapter sequences from high-throughput sequencing
654 reads. **17**, pp. 10-12 (2011).
655 59 Li, H. Aligning sequence reads, clone sequences and assembly contigs with BWA-MEM. *arXiv*
656 *preprint arXiv:1303.3997* (2013).
657 60 Shafer, R. W. Rationale and uses of a public HIV drug-resistance database. *The Journal of*
658 *infectious diseases* **194 Suppl 1**, S51-58, doi:10.1086/505356 (2006).
659 61 Okonechnikov, K., Conesa, A. & Garcia-Alcalde, F. Qualimap 2: advanced multi-sample
660 quality control for high-throughput sequencing data. *Bioinformatics (Oxford, England)* **32**,
661 292-294, doi:10.1093/bioinformatics/btv566 (2016).
662 62 Koboldt, D. C. *et al.* VarScan 2: somatic mutation and copy number alteration discovery in
663 cancer by exome sequencing. *Genome Res* **22**, 568-576, doi:10.1101/gr.129684.111 (2012).
664 63 Charles, O. J., Venturini, C. & Breuer, J. cmvdrg - An R package for Human Cytomegalovirus
665 antiviral Drug Resistance Genotyping. *bioRxiv*, 2020.2005.2015.097907,
666 doi:10.1101/2020.05.15.097907 (2020).
667 64 Perrier, M. *et al.* Evaluation of different analysis pipelines for the detection of HIV-1 minority
668 resistant variants. *PloS one* **13**, e0198334, doi:10.1371/journal.pone.0198334 (2018).
669 65 Goldstein, R. A., Tamuri, A. U., Roy, S. & Breuer, J. Haplotype assignment of virus NGS data
670 using co-variation of variant frequencies. *bioRxiv*, 444877 (2018).
671 66 Rozas, J. *et al.* DnaSP 6: DNA Sequence Polymorphism Analysis of Large Data Sets. *Mol Biol*
672 *Evol* **34**, 3299-3302, doi:10.1093/molbev/msx248 (2017).
673 67 Minh, B. Q. *et al.* IQ-TREE 2: New models and efficient methods for phylogenetic inference in
674 the genomic era. *bioRxiv*, 849372, doi:10.1101/849372 (2019).
675 68 Kalyaanamoorthy, S., Minh, B. Q., Wong, T. K. F., von Haeseler, A. & Jermiin, L. S.
676 ModelFinder: fast model selection for accurate phylogenetic estimates. *Nat Methods* **14**,
677 587-589, doi:10.1038/nmeth.4285 (2017).
678 69 Minh, B. Q., Nguyen, M. A. & von Haeseler, A. Ultrafast approximation for phylogenetic
679 bootstrap. *Mol Biol Evol* **30**, 1188-1195, doi:10.1093/molbev/mst024 (2013).
680 70 Tamura, K. & Nei, M. Estimation of the number of nucleotide substitutions in the control
681 region of mitochondrial DNA in humans and chimpanzees. *Mol Biol Evol* **10**, 512-526,
682 doi:10.1093/oxfordjournals.molbev.a040023 (1993).

71 Paradis, E., Claude, J. & Strimmer, K. APE: Analyses of Phylogenetics and Evolution in R language. *Bioinformatics (Oxford, England)* **20**, 289-290, doi:10.1093/bioinformatics/btg412 (2004).

689 **Table 1.** Regimens and viral load at final timepoint for all participants. Participants initiated and
690 maintained 1st-line regimens for between 1-10 years before being switched to 2nd-line regimens as
691 part of the TasP trial. Seven of the eight participants were failing 2nd-line regimens at the final
692 timepoint.
693

Participant	No. of timepoints	1st-line regimen	Time since initiation of 1st-line treatment (yrs.)	2nd-line regimen	Viral Load at final timepoint (copies/ml)
15664	6	d4T, 3TC, FTC	6.2	LPV/r, TDF, FTC	28655
16207	5	d4T, 3TC, NVP	5.9	LPV/r, TDF, FTC	56660
22763	8	d4T, 3TC, EFV	6.2	LPV/r, TDF, 3TC	15017
22828	6	d4T, 3TC, NVP	6.4	LPV/r, TDF, 3TC/FTC	947
26892	7	d4T, 3TC, EFV	6	LPV/r, TDF, FTC	12221
28545	5	TDF, FTC, EFV	1.3	LPV/r, AZT, 3TC	12964
29447	4	TDF, FTC, EFV	2.8	LPV/r, TDF, FTC	64362
47939	3	d4T, 3TC, EFV	10.1	LPV/r, AZT, 3TC/FTC	6328

694 **NRTI:** Stavudine, d4T; Lamivudine, 3TC; Tenofovir, TDF; Emtricitabine, FTC; Zidovudine, AZT. **NNRTI:**
695 Efavirenz, EFV; Nevirapine, NVP. **PI:** Lopinavir/ritonavir, LPV/r
696
697
698

699 **Table 2.** Nucleotide diversity between *gag*, *pol* and *env* reconstructed haplotype sequences from
700 three participants.
701

Participant	Diversity			
	Gene	**S**	**π**	**θ**
15664	*gag*	72	0.01721	0.01321
15664	*pol*	150	0.01489	0.01349
15664	env	190	0.02840	0.02241
16207	*gag*	86	0.02018	0.01543
16207	*pol*	192	0.01575	0.01675
16207	env	246	0.03173	0.02733
22763	*gag*	160	0.02265	0.02608
22763	*pol*	292	0.01724	0.02323
22763	env	251	0.02498	0.02558

702 Diversity (**S** = number of segregating sites, **π** = nucleotide diversity, **θ** = Watterson genetic diversity)
703 rates
704
705
706

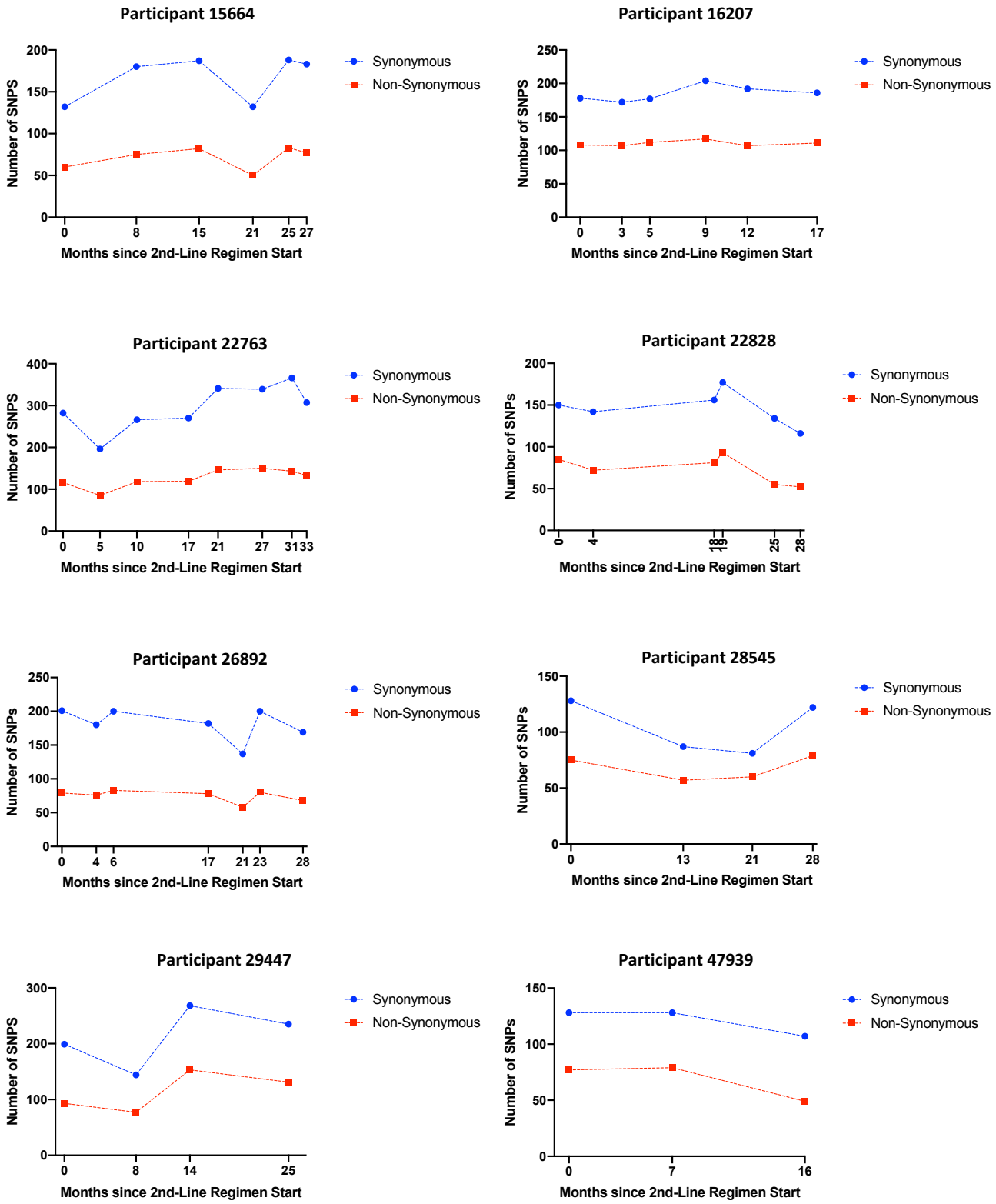

Figure 1. Measure of divergence from the SNPs relative to subtype C reference strain at successive timepoints in eight individuals under non-suppressive ART. These data were for SNPs detected by Illumina NGS at a threshold of 2% abundance. Sites in this analysis had coverage of at least 10 reads.

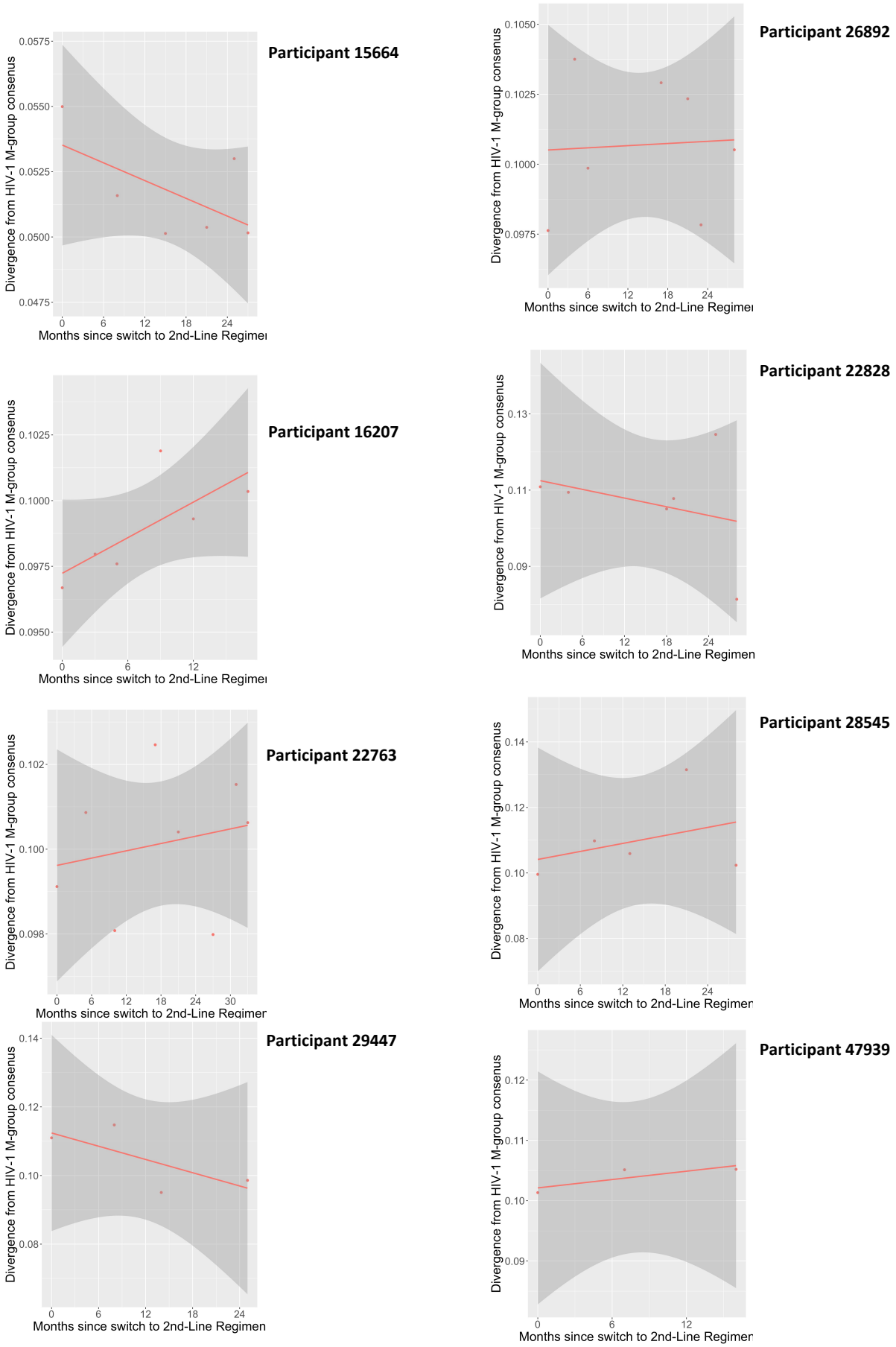

Figure 2. Divergence under non suppressive ART: Linear regression of average pairwise distance relative to a reconstructed subtype M consensus. Average pairwise distances were estimated under a TN93 substitution model and reveal increase divergence from from the initial samples. The 2002 HIV-1 subtype M group consensus sequences (Alignment ID: 102CG1) was downloaded and an overall ancestral consensus created from this using Geneious Prime v2021.1. This was used as a proxy for an ancestral HIV-1 group M sequence, which allowed us to determine if throughout ongoing treatment, the virus was reverting to an ancestral/founder state or diverging further. Shaded regions represented 95% CI of the linear regression fit.

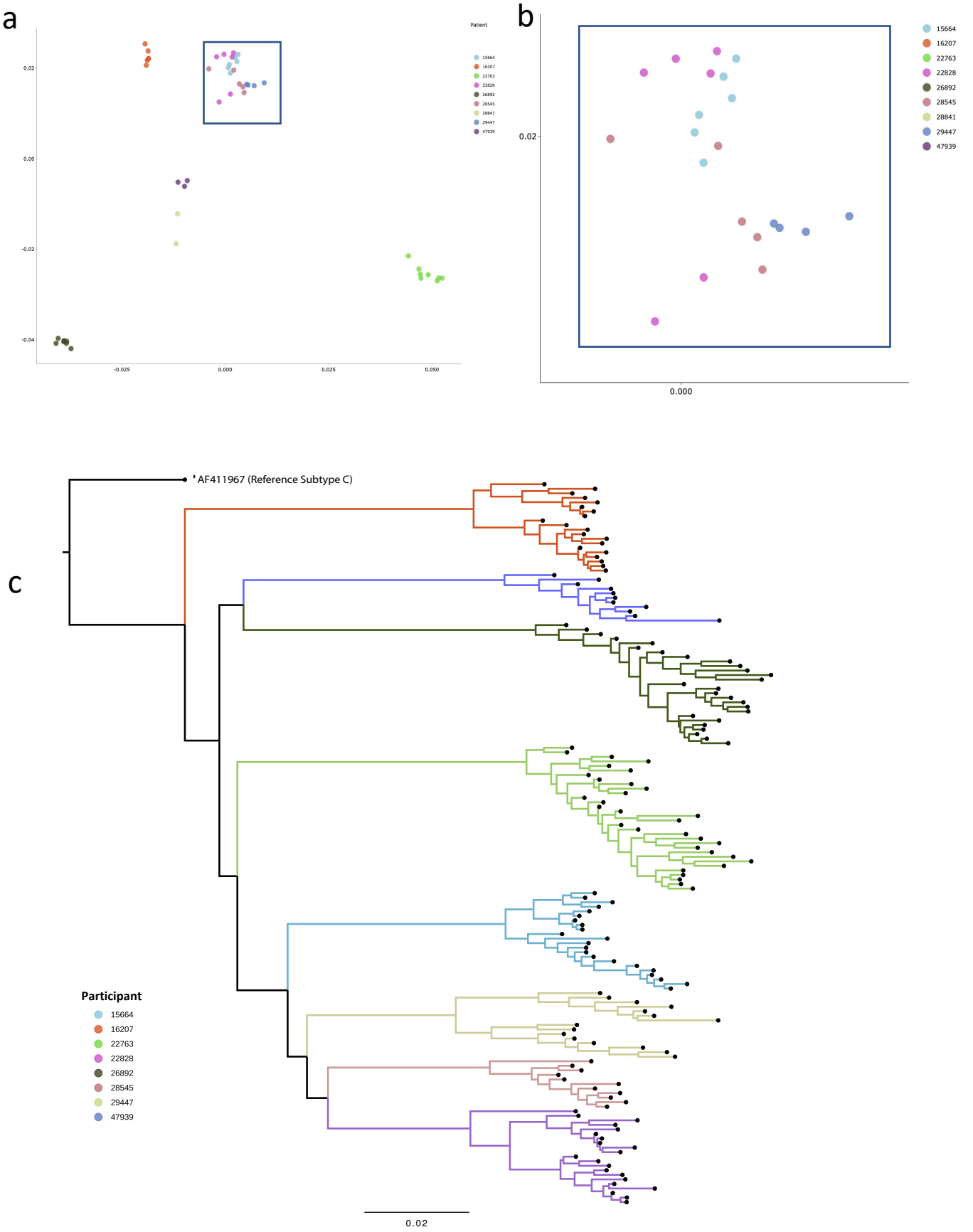

Figure 3. Multi-dimensional scaling showing A) clustering of HIV whole genomes from consensus sequences and **B) zoomed-in view of four participants with high intra-participant diversity.** Multi-dimensional scaling (MDS) were created by determining all pairwise distance comparisons under a TN93 substitution model, coloured by participant. **C) Maximum likelihood phylogeny of constructed viral haplotypes for all participants**. The phylogeny was rooted on the AF411967 clade C reference genome. Reconstructed haplotypes were genetically diverse and did not typically cluster by timepoint.

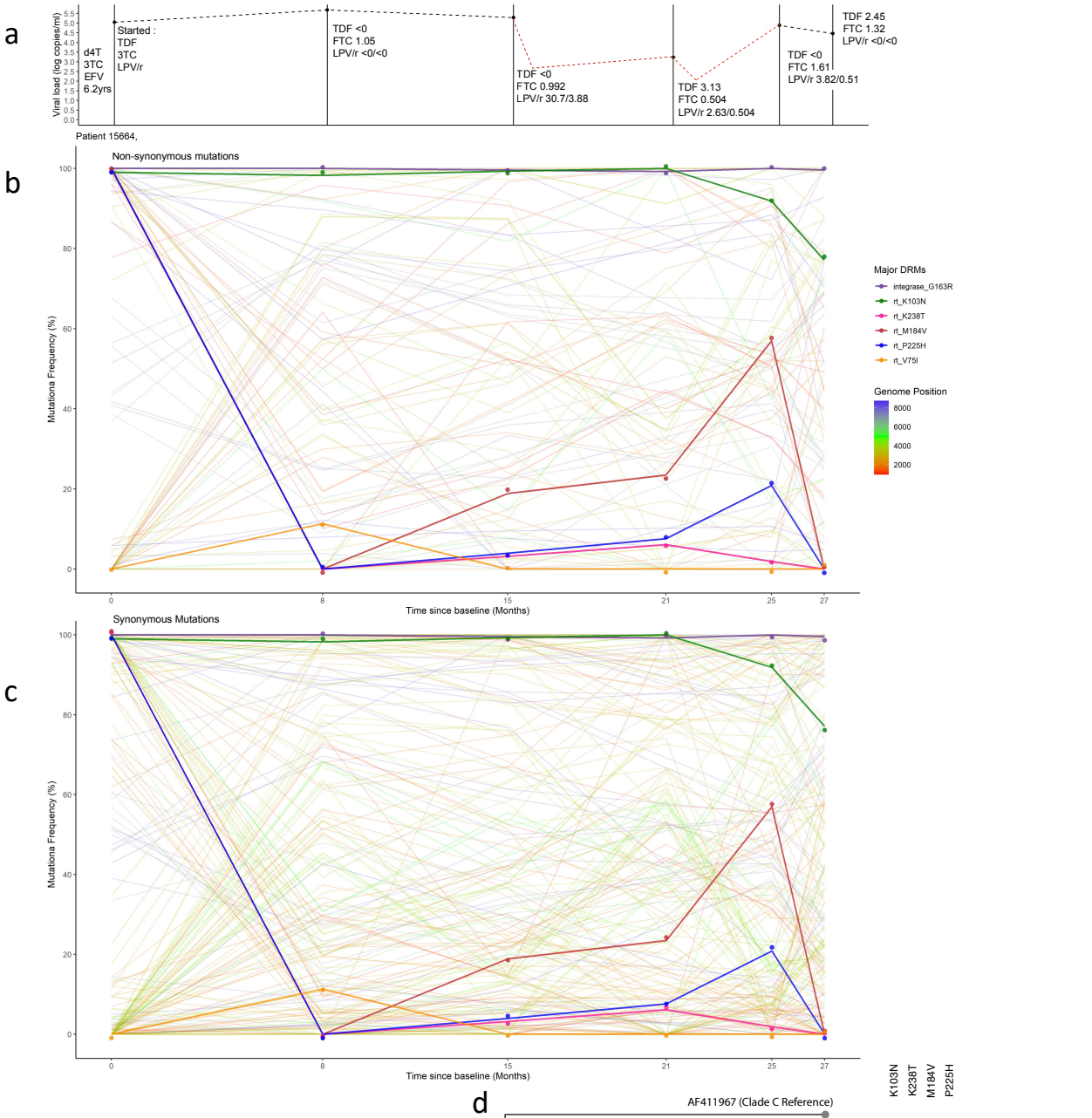

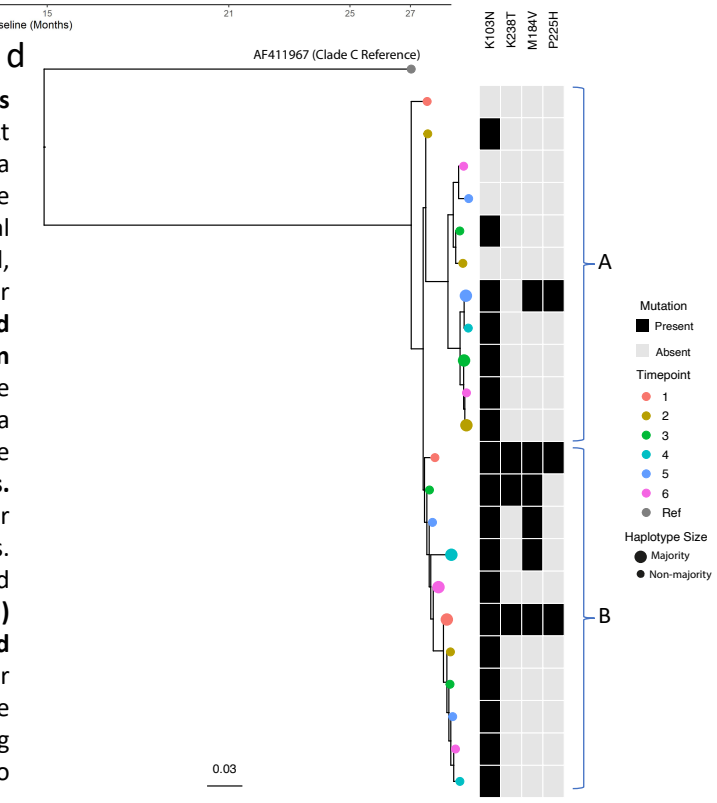

Figure 4. Drug regimen, adherence and viral dynamics within participant 15664. a) Viral load and drug levels. At successive timepoints drug regimen was noted and plasma drug concentration measured by HPLC (nmol/l). The participant was characterised by multiple partial suppression (<750 copies/ml, 16 months; <250 copies/ml, 22 months) and rebound events (red dotted line) and poor adherence to the drug regimen. **b) Drug resistance and non-drug resistance associated non-synonymous mutation frequencies by Illumina NGS.** The participant had large population shifts between timepoints 1-2, consistent with a hard selective sweep, coincident with the shift from 1st-line regimen to 2nd-line. **c) Synonymous mutation frequencies.** All mutations with a frequency of <10% or >90% at two or more timepoints were tracked over successive timepoints. Most changes were restricted to *gag* and *pol* regions and had limited shifts in frequency i.e. between 20-60%. **d) Maximum-likelihood phylogeny of reconstructed haplotypes.** Haplotypes largely segregated into two major clades, those with the NNRTI mutation K103N and those without. Majority and minority haplotypes, some carrying lamivudine resistance mutation M184V. Clades referred to in the text body are shown to the right of the heatmap.

a

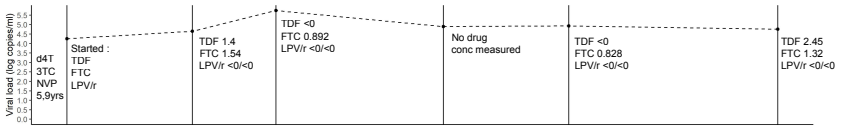

b

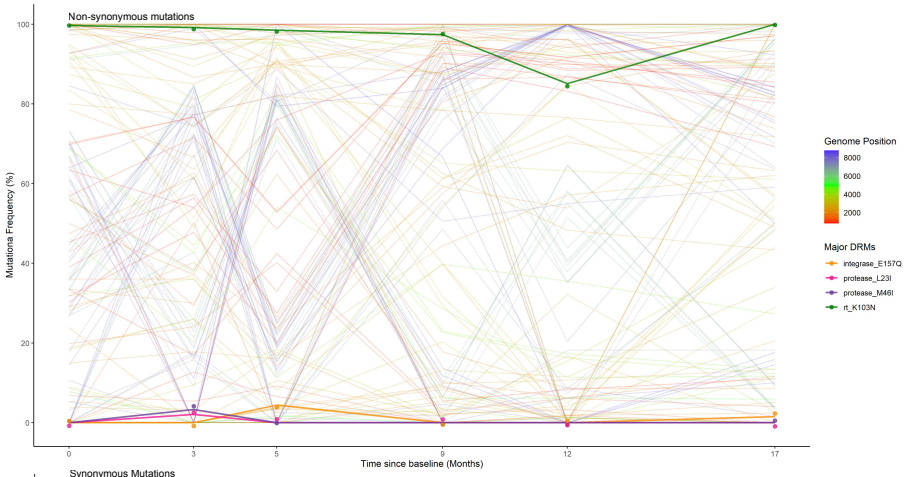

c

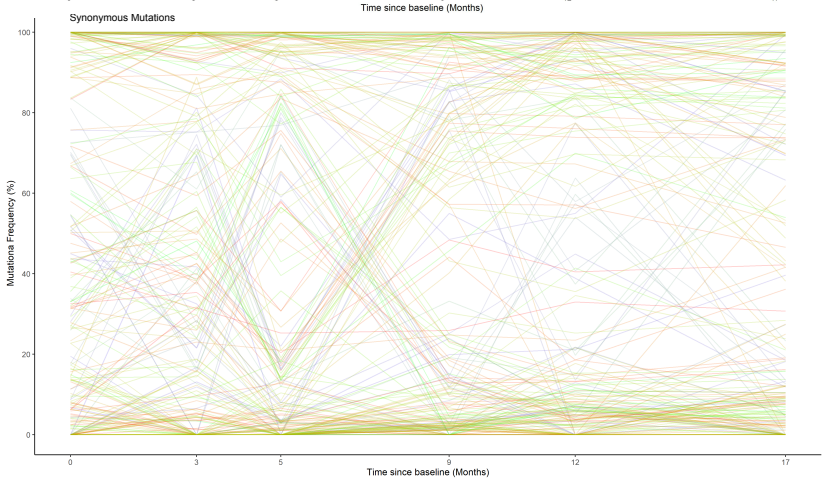

d

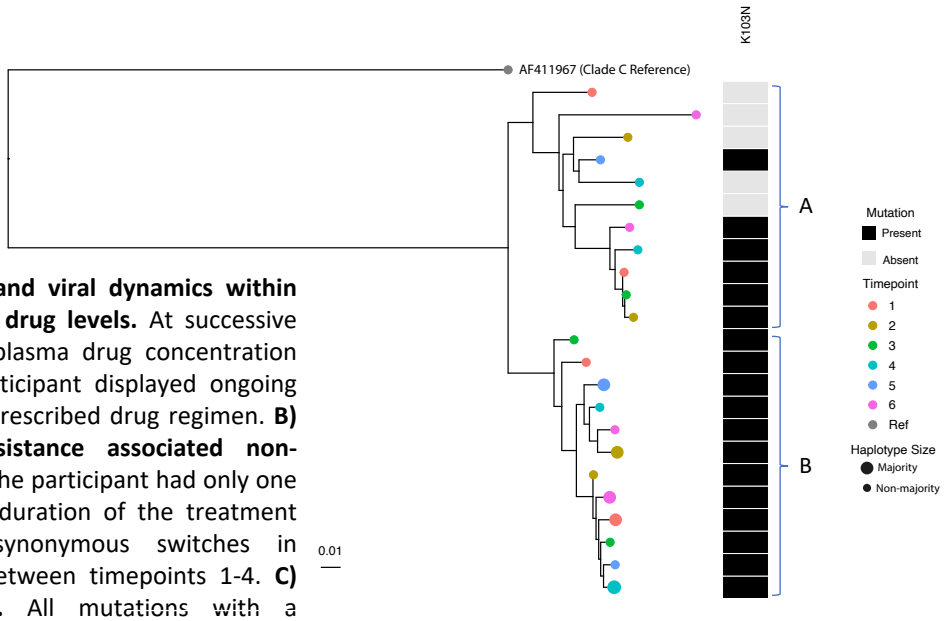

Figure 5. Drug regimen, adherence and viral dynamics within participant 16207. A) Viral load and drug levels. At successive timepoints regimen was noted and plasma drug concentration measured by HPLC (nmol/l). The participant displayed ongoing viraemia and poor adherence to the prescribed drug regimen. **B) Drug resistance and non-drug resistance associated non-synonymous mutations frequencies.** The participant had only one major RT mutation - K103N for the duration of the treatment period. Several antagonistic non-synonymous switches in predominantly *env* were observed between timepoints 1-4. **C) Synonymous mutation frequencies.** All mutations with a frequency of <10% or >90% at two or more timepoints were followed over successive timepoints. In contrast to non-synonymous mutations, most synonymous changes were in *pol*, indicative of linkage to the env coding changes. **D) Maximum-likelihood phylogeny of reconstructed haplotypes.** Haplotypes were clearly divided by a bifurcation; each clade contained haplotypes from all timepoints, suggesting lack of hard selective sweeps and intermingling of viral haplotypes with softer sweeps. that most viral competition occurred outside of drug pressure.

a

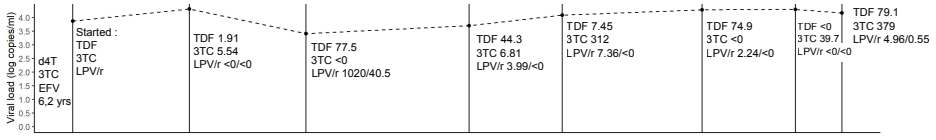

b

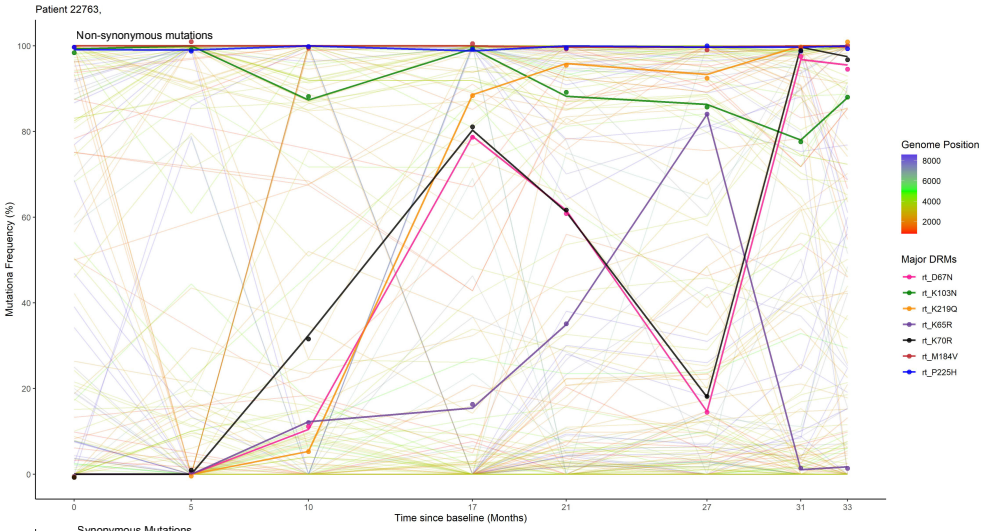

c

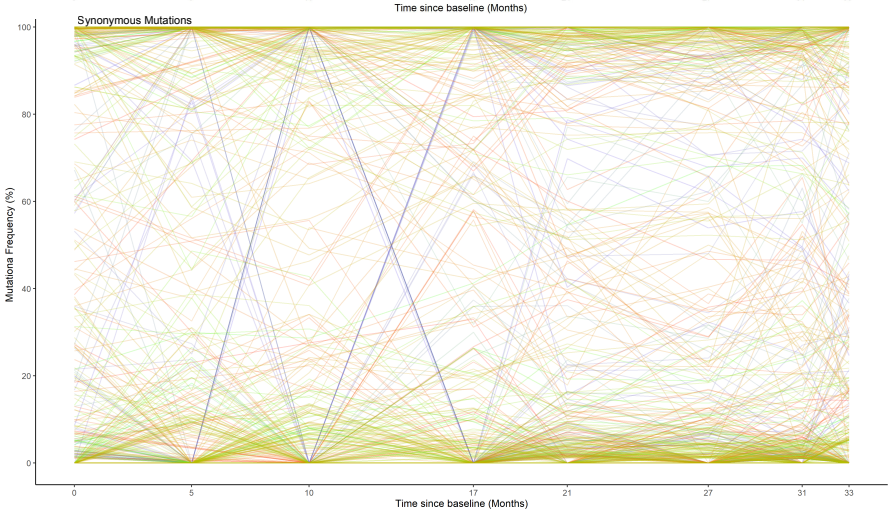

d

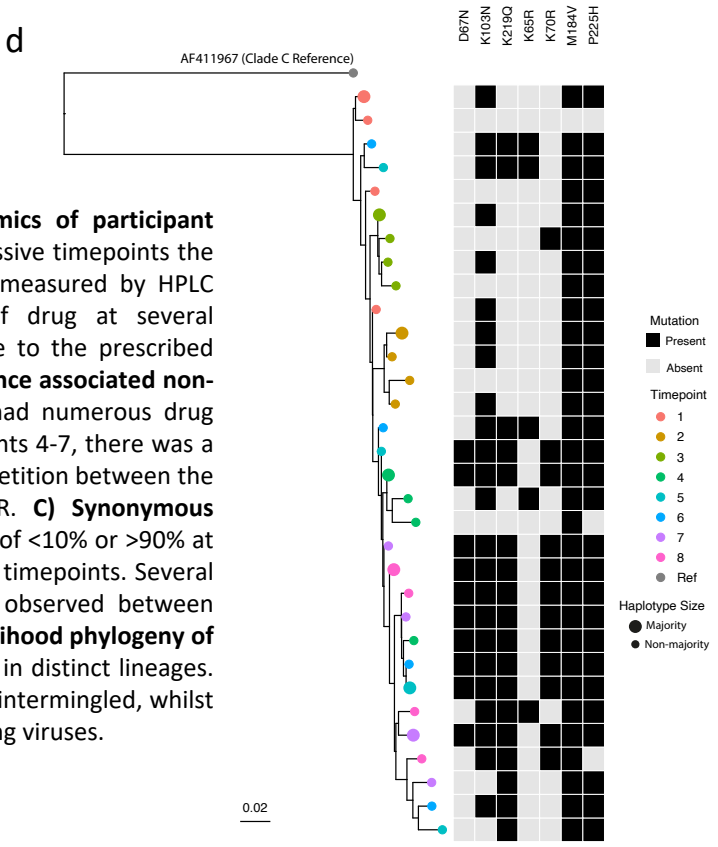

Figure 6. Drug regimen, adherence and viral dynamics of participant 22763. A) Viral load and regimen adherence. At successive timepoints the regimen was noted, and plasma drug concentration measured by HPLC (nmol/l). The participant had therapeutic levels of drug at several timepoints (3, 5 and 8), indicating variable adherence to the prescribed drug regimen. **B) Drug resistance and non-drug resistance associated non-synonymous mutation frequencies.** The participant had numerous drug resistance mutations in dynamic flux. Between timepoints 4-7, there was a complete population shift, indicated by reciprocal competition between the RT mutations K65R and the TAMs K67N and K70R. **C) Synonymous mutations frequencies.** All mutations with a frequency of <10% or >90% at two or more timepoints were followed over successive timepoints. Several *env mutations* mimicked the non-synonymous shifts observed between timepoints 2-4, suggestive of linkage. **D) Maximum-likelihood phylogeny of reconstructed haplotypes.** timepoints 1-3 were largely in distinct lineages. In later timepoints, from 4-8, haplotypes became more intermingled, whilst maintaining antagonism between K65R and K67N bearing viruses.